Revisiting regulatory decoherence: Accounting for temporal bias in a co-expression analysis reveals novel candidates controlling environmental response

Haoran Cai[1], David L. Des Marais[1]

[1]Department of Civil and Environmental Engineering, MIT.
15 Vassar St., Cambridge, MA, 02139 USA

Submitted as a Research Article

Number of references: 105 references

KEYWORDS: Network rewiring; Temporal transcriptome; Dynamic correlation; Regulatory coherence; Dynamic regulatory map

Abstract

Transcriptional Regulatory Networks (TRNs) orchestrate the timing, magnitude, and rate of organismal response to many environmental perturbations. Regulatory interactions in TRNs are dynamic but exploiting temporal variation to understand gene regulation requires a careful appreciation of both molecular biology and confounders in statistical analysis. Seeking to exploit the abundance of RNASequencing data now available, many past studies have relied upon population-level statistics from cross-sectional studies, estimating gene co-expression interactions to capture transient changes of regulatory activity. We show that population-level co-expression exhibits biases when capturing transient changes of regulatory activity in rice plants responding to elevated temperature. An apparent cause of this bias is regulatory saturation, the observation that detectable co-variance between a regulator and its target may be low as their transcript abundances are induced. This phenomenon appears to be particularly acute for rapid onset environmental stressors. However, exploiting temporal correlations appears to be a reliable means to detect transient regulatory activity following rapid onset environmental perturbations such as temperature stress. Such temporal correlation may lose information along a more gradual-onset stressor (e.g., dehydration). We here show that rice plants exposed to a dehydration stress exhibit temporal structure of coexpression in their response that can not be unveiled by temporal correlation alone. Collectively, our results point to the need to account for the nuances of molecular interactions and the possibly confounding effects that these can introduce into conventional approaches to study transcriptome datasets.

1 Introduction

Living organisms evolve to maximize their individual performance under dynamically changing environments. Transcriptional regulation plays a fundamental role in the behavior of cells responding to external and internal environmental cues, and is aberrant in many diseases (Lee and Young 2013). Networks comprised of directed links between pairs of genes are termed "Transcriptional regulatory networks" (TRNs), and are often used by organisms to coordinate cellular, physiological, and developmental response to the varying environment. TRNs orchestrate the timing and rate of genome-wide gene expression

plastic responses (Gibson 2008) and, as such, a long-standing goal in molecular biology is to understand functional linkages between regulatory architectures in TRNs and the dynamic behavior of organisms (Smith 1990). Transcription factors (TFs) are key nodes in TRNs that regulate the expression of other genes (Buchanan et al. 2010), coordinating the entire transcriptional program. Accordingly, TFs remain appealing therapeutic and engineering targets for disease (Neef et al. 2011, Spampanato et al. 2013, Neef et al. 2010, Cuadrado et al. 2018) and stress tolerance for crop production (Wang et al. 2016, Lan Thi Hoang et al. 2017). While decades of research provide insight into the basic mechanics of transcription, relatively little is known about how TFs function collectively in intricate regulatory networks in multicellular eukaryotes to achieve complex biological outputs in response to dynamic environments. As large-scale high-throughput -omic data are now readily generated for many ecologically and economically important species (Chen et al. 2020, Li et al. 2019, Müller et al. 2017, Rastogi et al. 2018, Wilkins et al. 2016), data-driven methods are needed for discovering key responsive TFs and for understanding how such TFs drive dynamic responses to the environment.

Many regulatory interactions in TRNs are context-dependent (Dunlop et al. 2008, Luscombe et al. 2004). Environmental cues can affect the behavior of regulators (e.g., by changing their abundance or their binding affinity to target DNA sequences), and thereby change the transcriptional output and regulatory interactions with other genes. For instance, an interaction can be inactive simply because the concentration of the regulator is outside its effective range for the target (Dunlop et al. 2008). Notably, even if a regulatory interaction is activated, its regulatory activity can be low as the dose-response curve may be under a saturated regime in which additional units of the regulator do not result in changed activity of its target(s). Alternatively, interactions may be inactive as a result of the chromatin state of target genes, the post-translational modification of the regulator itself, the presence of inhibitory factors, or the absence of co-factors (Toledo and Wahl 2006, Piggot and Hilbert 2004).

Identifying transient changes in regulatory activities (i.e., detecting responsive regulatory interactions) upon environmental perturbation is critical to understand how genes and proteins modulate cellular and organismal responses to variable environments. One approach to directly estimate the strength of regulatory interactions is to use ChIP-seq. However, genome-wide ChIP-seq for hundreds of transcription factors across multiple

conditions is costly, technically challenging, and therefore currently inaccessible in most organisms. Few dynamic transcription factor binding studies have been undertaken, with many of these focused on a small set of TFs or only assaying physical binding under a specific environmental condition (Chang et al. 2013, Ni et al. 2009, Garber et al. 2012, Zinzen et al. 2009). Numerous computational studies have also addressed the dynamic nature of TRNs, e.g., by exploiting static network priors and gene expression profiles to identify subnetworks activated by environmental perturbation (Luscombe et al. 2004, Scott et al. 2005, Ernst et al. 2007). Gene co-expression analysis is another widely used tool to identify regulatory interactions that are activated/deactivated following perturbations. For example, differential co-expression analysis has been used to identify gene function underlying differences between healthy and disease samples (Amar et al. 2013, Hu et al. 2009, Kostka and Spang 2004, Hudson et al. 2009, Fiannaca et al. 2015, Bhar et al. 2013, Gao et al. 2016), between species (Ferrari et al. 2018, Gao et al. 2012, Monaco et al. 2015, Ruprecht et al. 2017*a*,*b*), or under different environmental conditions (Yan et al. 2019, Lea et al. 2019). The most frequently used programs for co-expression analysis are WGCNA (Langfelder and Horvath 2008), DICER (Amar et al. 2013) and DiffCoEx (Tesson et al. 2010); often, however, the ease of performing analyses on these platforms obscures the assumptions they make about regulatory interactions. Because the ultimate aim in deciphering complex biological processes is the discovery of the causal genes and regulatory mechanisms controlling biological processes, it is critical to understand possible biases and confounding factors during co-expression analysis.

Here, we exploit the temporal component of gene co-expression to characterize the dynamic regulatory map and co-expression patterns in a static network prior. The static network prior was previously derived from ATAC-seq and known TF-binding motifs (Wilkins et al. 2016). Our analysis and simulation imply that multiple types of temporal bias can occur when analyzing gene expression data: First, sampling time points may not be appropriate/sufficient to capture the transient response of genes (Bar-Joseph et al. 2012). Second, population coexpression may bias to capture transient induction of regulatory activities when under a regulatory saturated regime, thereby fail to detect responsive regulatory interactions. Because even if the sampling time point has capture the transient reponse of single gene expression, under a regulatory saturated regime, the duration of high regulatory activity can be short. Therefore, it is highly likely that the sampling

time points can not detect the transient increases of regulatory activity. Third, temporal correlation can alleviate the second temporal bias. However, while the temporal correlation can detect whether a certain regulatory interaction is induced or not, it is unable to track the temporal evolution of the regulatory activity. By analyzing the co-expression pattern upon elevated temperature and dehydration process, we found that for rapid onset environmental stressors (e.g., heat shock), temporal correlation is more robust than population correlation in revealing transient response of regulatory activity and identifying responsive regulatory interactions. We thus provide a possible explanation for a seemingly inconsistent result from a recent study, which demonstrated that internal and external stressors can cause regulatory "decoherence" (lower correlation) (Lea et al. 2019). On the other hand, for mild and gradual stressors (e.g., drying for plants), the temporal correlation is relatively rough and incapable to unveil the full picture and complicated dynamics during perturbations. Extensive efforts have been made to exploit the so-called "fourth dimension" of response — time — to better understand the dynamics of TRNs and to identify putative signaling pathways or key regulatory genes (Bechtold et al. 2016, Yeung et al. 2018, Varala et al. 2018, Zander et al. 2020, Song et al. 2016, Greenham et al. 2017, Windram et al. 2012, Gargouri et al. 2015, Alvarez-Fernandez et al. 2020). Our work reinforces the importance of temporal dynamics and reveal the signature of regulatory saturation, a specific confounding factor which may lead to bias in reconstructing dynamic regulatory maps, pointing to the need to account for the possibly confounding effects that can introduce into conventional approaches to study transcriptome datasets.

2 Results

2.1 Temporal bias in revealing dynamic regulatory interactions

We first evaluate the overall dynamic patterns of pairwise regulatory interactions by calculating the Maximum Cross Correlation (MCC, see Methods) for each pair of transcripts in a static network reported previously (Wilkins et al. 2016). The data comprise four rice cultivars grown under control, dehydration stress, or elevated temperature conditions; here we analyze the data by condition over a time duration of 135 minutes following the incidence of stress. Calculated Maximum Cross Correlations (MCC) from all four

cultivars were merged stress-wise. We set a threshold of 0.69 (p-value = 0.01) together with a fold-change cutoff (Fig. 2) according to the MCC under controlled conditions as the cutoff for the activation of regulatory interactions. We use the terms regulatory coherence and decoherence to mean increasing or decreasing co-expression, respectively. Coherence in our analyses is reflected by higher MCCs under heat or dehydration stress conditions when compared to control samples, as imposed by Wilkins et al. (2016).

The distributions of MCC (Figure 1) reveal that stressful environments increase the coexpression strength among measured transcripts in the network prior. The distribution of the MCC under heat (Kolmogorov-Smirnov test statistic D = 0.0445, p-value $< 2.2 \times 10^{-16}$) and drought (Kolmogorov-Smirnov test statistic D = 0.0929, p-value $< 2.2 \times 10^{-16}$) conditions are significantly different from the control condition. We identified significant TF-gene interactions in stressful conditions which were not observed in the controlled condition, and vice versa. We found greater support for the former number: out of 38127 total interactions in the network prior, 496 and 839 pairs transition to active pairs in heat and drying stress, respectively (light blue points in Fig. 2A and 2B), whereas only 91 and 115 of them transition to inactive pairs under heat or drying, respectively. The observation of regulatory coherence is robust to various thresholds for activation (Fig. S1 and Fig. S2). Collectively, these results suggest a strong bias toward regulatory coherence in this rice expression dataset.

Our observation that co-expression increases with the onset of stress (regulatory coherence) is seemingly inconsistent with a recent study which used gene expression profiles collected from human monocytes exposed to a stress in vitro to calculate the differential population correlation among pairwise transcripts (Lea et al. 2019). Lea et al. found evidence supporting regulatory decoherence following perturbation. To explore the possible role of statistical methodology to explain the differing results of our two studies, we conducted a cross sectional analysis by using the above rice gene expression data and static network prior. Strikingly, for heat shock stress response, population-level coexpressions show little or no evidence of regulatory coherence under stress (Fig. 2C, S1 and S2). At many time points, the distributions of correlation coefficients under the stress condition are skewed towards regulatory decoherence (Fig. S5). An even more striking contrast is from the so-called heat shock regulon (Fig. 3A and Fig. 3B), formed by all the Heat Shock Family TFs and interactions with their target genes in the static network prior. On the other hand,

for drought stress response, the population coexpressions show regulatory coherence at a few time points (Fig. S6). One confounding factor that may be involved, as pointed out by Lea et al. (2019), Parsana et al. (2019), is technical and unwanted biological covariates (e.g. genotype, cultivar effect) which may lead to spurious correlations. To remove the genotypic effect, we use another dataset from *Brachypodium* with larger number of replicates for drought treatments (Yun et al. 2021, in prep). We still observed regulatory coherence in drought responses after removing unwanted covariates (Fig. S5). We further hypothesize that, regulatory saturation (Fig. 3C) may contribute to the temporal bias we observed in the heat response.

2.2 Regulatory saturation as a cause for temporal bias

Through a simple mathematical model, we illustrate how regulatory saturation may be a confounding factor for identifying responsive links. We contrast the outcomes of population-level metrics with our measure based on cross-correlation. A typical regulation function between a TF and a target gene (modeled as a dose-response curve) can be characterized as a Hill function (Alon 2019, Chu et al. 2009), which is nonlinear (cooperative binding mode with Hill coefficient $n > 1$) as shown in Fig. 4C and F (grey line). Two perturbation regimes are considered: A saturated regime in which additional TF transcripts beyond some concentration threshold fail to induce additive responses in their target genes, and a non-saturated regime characterized as the portion of a dose-response curve in which additional TF transcripts are associated with increased expression of their targets. We assume that the external perturbation modulates gene expression dynamics by the signal S_x. Smaller K_x and larger Hill coefficients increase the probability of saturation of regulation after environmental perturbation. The saturation of the regulation effectively masks the differential regulatory interaction upon perturbation, even if the TF X is nominally an environmentally induced activator of the gene Y. In addition, two possible external perturbation regimes are simulated (Fig. 4B): press perturbation and pulse perturbation, which differ in the duration of the perturbation imposed on the given regulatory pair. If the upstream signal for a TF-gene pair has the property of adaptation, the signal induction may only last for a short period of time. Adaptation here is defined

by the ability of circuits to respond to input change but to return to the pre-stimulus output level, even when the input change persists (Ma et al. 2009, Briat et al. 2016).

Fig. 4E shows that, under a saturated regime, the population-level correlation between X and Y can become even lower under a perturbation, despite the fact that the interaction between X and Y is activated by an environmental perturbation. On the other hand, under a non-saturated regime, the population-level correlation between the regulator and its target increases (Fig. 4H). It should be noted that under a non-cooperative binding mode (e.g., Hill coefficient equals 1), the population-level correlation will decrease independently under the saturation regime. Therefore, how population-level correlations change relies upon whether a given transcriptional interaction is under a saturated regime or not; population-level correlations can fail to capture transient environmentally responsive links. Such bias can be termed the temporal bias (Yuan et al. 2021). However, the temporal correlation between TF X and target gene Y is sensitive enough to characterize the environmentally induced activation under both saturated and non-saturated regimes induced by either press or pulse perturbation by S_x (Fig. 4D and G). These results highlight the likely incidence of false negatives in identifying responsive gene interactions when relying on population-level correlations. While Bar-Joseph et al. (2012) has argued that temporal information enable the identification of transient transcription changes, our results suggest that even if transient transcriptional changes are captured the population correlation analysis can be biased to identify responsive links, reinforcing the importance of using temporal dynamics.

However, despite that using temporal correlation can robustly detect transient responses of regulatory activity, it blurs the complicated dynamics of regulatory activity over the time course: you can not track the real-time regulatory activity (Fig. 4D and Fig. 4G). Conversely, population correlation over time can reflect the dynamic activity of a regulatory interaction. In other words, the reason population correlations may fail to capture transient responses of regulatory activity is that population correlations are capable of detecting real-time regulatory activity, whereas the temporal correlation is not. That is to say, whenever a low population coexpression corresponds to a low activity of the link even if a link is activated and responsive towards the treatment. The low activity of a regulatory interaction means additional regulators will not induce more expression of its target gene. Therefore, under a saturated regime, either low or high regulator

abundance lead to inactive regulatory interaction and low regulatory activity. In the following sections, we will leverage the temporal component of stress response by using temporal correlations and population correlations over time.

2.3 Temporal correlations prioritizing novel candidates in regulating stress responses

We next analysed dynamic transcriptional rewiring through temporal correlation. We examined whether certain TF families affect the activation of regulatory interactions (Fig. S10) and find that, as expected, many TFs with high differential mean MCC in the heat-stress data set are annotated as Heat Shock transcription Factors (HSFs).

Inspecting the relationship between differential gene expression and the differential activity reveals that several known HSFs do not independently show strong expression response to the stressor but do, however, show a clear response according to the differential activity calculated by the temporal correlation of a TF with its target genes. We also find several interesting candidate TFs outside of the HSF family which have high differential regulatory scores but little or no apparent differential expression in pairwise contrasts between control and treatment conditions (Fig. 5A). In the heat data set, the TF OsTCP7 has a differential regulatory score of 0.54 but was not identified as differentially expressed by Wilkins et al. (Wilkins et al. 2016). TCPs are broadly involved in regulating cell proliferation and growth (Martín-Trillo and Cubas 2010) and so OsTCP7 may be an interesting candidate for functional validation in the context of heat stress response.

While the HSF TFs comprise a gene family and are generally interpreted as coordinating plant response to heat stress (von Koskull-Döring et al. 2007), the regulatory control of response to soil drying is more distributed among diverse gene families and regulatory pathways (Joshi et al. 2016, Manna et al. 2020, Des Marais et al. 2012). Our analysis of the drought response data identified several TFs with previously demonstrated roles in rice dehydration response. These include HOX24 (Bhattacharjee et al. 2021) and ZFP182 (Huang et al. 2012), both of which were also found by Wilkins et al. to show a strong differential response. Several interesting candidates emerge among the list of TFs which have high differential regulatory score but low differential expression response.

One such gene is PIF-Like 12 (Nakamura et al. 2007) which, to our knowledge, has no known role in dehydration response but is paralagous to OsPIL1 which integrates cues from the circadian clock and dehydration signaling to control internode elongation in rice (Todaka et al. 2012). Additional candidate genes with high regulatory scores under elevated temperature or dehydration stress are shown in Table S1 and S2. We hypothesize that the differential activity calculated by temporal correlation could be used to identify novel stress-responsive regulators.

2.4 Dynamic TF activity under dehydration conditions reveal signal propagation upon environmental perturbations

The stochastic simulation suggests that population correlations may be suitable for estimating the activity of a regulatory link even though they may miss transient interaction changes (Fig. 4, Dunlop et al. 2008). On the other hand, temporal correlation is capable of capturing transient responses of regulatory activities but may miss some important information over the whole time course of treatment since it only gives a single summarized value without possible temporal fluctuation during the time course, leading to a different type of temporal bias. In the rice data set considered here, the temporal correlation does not show a strong signal in detecting drought-responsive TF (Fig. 5B). To explore the possible reason for this discrepancy compared to heat response (Fig. 5A), we next analyze TF activities over time under drought treatment by using the population correlation. We find that the population correlation can indeed unveil the dynamic regulatory map in additional layers through temporal correlation.

We first construct a network hierarchy in the TF-only subnetwork from the network prior (Fig. 6A). Since the network has feedback loops (See Supporting Information), we used a generalized bottom-up approach (Yu and Gerstein 2006). In essence, we define all TFs that do not regulate any other TFs as bottom TFs and define the level of the remaining TFs by their shortest distance to a bottom TF. Caveats and other alternative approaches constructing hierarchy are discussed in the Supporting Information. 89 of the 357 TFs in the network neither regulate other TFs nor are themselves regulated by other TFs; thus, these 89 TFs are not present in the generalized hierarchical structure. The regulatory signal can be amplified and propagated in a top-down manner, which can be observed in

the mean expression level and temporal fluctuation of TFs in the generalized hierarchy, in which TFs in the top layers show lower expression and weaker fluctuations as compared to the bottom TFs (Fig. 6B). Such evidence implies that differential expression analysis may bias towards bottom TFs and other downstream target genes which likely have higher transcript abundances and higher fluctuations that provide the variance necessary to infer signatures of environmental response.

We next examined dynamic TF activities after the drought treatment. TF activity is calculated as the average coexpression level (PCC) with all of its target genes in the static network prior we used in previous sections. We also filtered the TF pools by removing non-responsive TF (although this filtering step has only a moderate effect on the results; Fig S11). Note that many responsive TFs are non-DE genes, suggesting that many transcriptional regulations can occur without significantly changing abundance of regulators. And, as expected, genes that cannot be detected by differential expression but are identified as responsive TFs by their activities do not fall into the bottom layer of the hierarchy. This observation suggests that there is signal amplification through the transcriptional cascade: higher layer TFs and master regulators are more likely to control downstream genes without a detectable change in their own transcript abundances in the data available.

Overall, we observed two regulatory waves for temporal activities (Fig. 6C), which were not prominent in the temporal expression profile considered above (Fig. 6B). We speculate that these two waves may represent distinct phases rice response to the sever drying imposed, perhaps before and after turgor loss occurs (Buckley 2005). We note that Wilkins et al. observed two distinct phases with respect to carbon assimilation, with a steep decline in assimilation during the initial phase followed by a slower decline beginning around the 60th minute following onset of dehydration stress (Wilkins et al. 2016). We next clustered short time series of single TF activity with the help of STEM (Ernst and Bar-Joseph 2006), which does unsupervised clustering and infers two regulatory waves along with putative drivers of each wave. We found four distinct groups of TFs (Fig. 6C insets, Fig. 6D and Fig. 6E). Fig. 6D presents a group of TFs with continuously increasing activity over the time course. Fig. 6E, top left inset of Fig. 6C and bottom right inset of Fig. 6C show groups driving both waves, the first wave and the second wave alone respectively. The group of TFs putatively driving the second wave contains two

TFs: RR21, from the bottom layer, encodes a putative response regulator involved in cytokinin signaling (Tsai et al. 2012), while GL1A, from the top layer, encodes an ortholog of the Arabidopsis R2R3 MYB transcription factor GL1 (Zheng et al. 2021). A cascade of TFs representing the shortest path between these two TFs were identified in the TF-only network prior (Fig. 6C).

3 Discussion

Studies in human disease and plant and animal stress response frequently use genome-wide gene expression data to study changes in co-expression changes and network rewiring in response to environmental perturbation (Fukushima 2013, Southworth et al. 2009, de la Fuente 2010, Amar et al. 2013, Choi et al. 2005, Kostka and Spang 2004, Deng et al. 2015, Yan et al. 2019, Cho et al. 2009, Fukushima et al. 2012, de la Fuente 2010, Zeisel et al. 2015, Bhar et al. 2013, Fiannaca et al. 2015). Ultimately, the aim of such studies is to identify the cellular basis of environmental responses as a means to understand abnormal regulation in disease states, to design medical interventions (Southworth et al. 2009, de la Fuente 2010, Amar et al. 2013, Kostka and Spang 2004) and breeding strategies (Fukushima et al. 2012), or to parameterize models of molecular evolution (Wray et al. 2003). However, many past studies have relied on population-level statistics to estimate pairwise gene co-expression relationsips to detect what are, very often, transient gene-gene interactions (Cortijo et al. 2020, Fukushima et al. 2012, Deng et al. 2015, Lea et al. 2019). While statistically straightforward, such widely used population-based methods likely miss many dynamic interactions which drive organismal response, thereby generating an incomplete picture of these complex systems. First, without a static transcriptional network prior, generating a pairwise gene co-expression network and detecting responsive links can lead to false positives as many of links may be indirect and not involve any causal regulatory relationship (Feizi et al. 2013, Barzel and Barabási 2013). Second, population-level statistics are often confounded by individual covariates such as genotype, age, and sex (Parsana et al. 2019, Lea et al. 2019). Third, even within an isogenic homogeneous population, cross sectional population correlations may be confounded by switch-like transitions and ultrasensitivity in gene regulation, thereby failing to characterize the dynamic network rewiring (Fig. 3 and Fig. 4). On the other hand, temporal correlation

can fail when we aim to track real time regulatory activity (Fig. 4). Our results reinforce the importance of temporal component in gene expression (Bar-Joseph et al. 2012). Additionally, even with the temporal information in hand, one should analyze the data according to its specific aim: detecting responsive links (Fig. 5) or tracking regulatory activities (Fig. 6).

In the present study, we implemented a stochastic simulation of a simple regulatory model under two perturbation regimes. We show that, under a cooperative binding mode, the population-level co-expression changes of an environmentally induced link depend upon whether the gene regulation is under a saturated regime or not. Our results also indicate that while population-level correlations may be confounded by saturated regulation, temporal correlations of gene expression time series are robust in both regimes. Hence, while temporal co-expression tends to be coherent upon environmental perturbation, whether the co-expression measured using population statistics becomes coherent or decoherent may depend upon the specific parameters of a given gene pair and the environmental condition. Such potential temporal bias that occurs when using cross-sectional data (also as population-level correlation) has been established in the medical literature (Yuan et al. 2021). Notably, regulatory saturation behaviors have been detected experimentally. For example, by measuring the activity of 6500 designed promoters using a fluorescence reporter, van Dijk and colleagues (van Dijk et al. 2017) found that target promoter activities can become saturated with the increasing abundance of the active form of TFs, and that the pattern becomes more pronounced with more binding sites or higher binding affinity.

Importantly, we found that under heat stress the temporal bias is prominent, whereas under drought stress such bias is not. Furthermore, when removing other covariates (genotypic variation), drought treatments lead to clear patterns of regulatory coherence with population correlation, which suggests that regulatory saturation is relatively less common during drought response. We reason that such a distinct pattern reflects the varying etiology of response to different stressors and is largely attributable to the internal environment an organism experienced during stress onset: drying is a fairly gradual process internally while the heat treatment is a shock – particularly as implemented in laboratory settings – and more sudden process for an organism. We thus suspect that the drought response is under an unsaturated regime in the rice data and is relatively more

mild compared to the heat response. Conversely, the heat shock treatment is intense and under the saturated regime. Environmental responses that show regulatory saturation may not have been optimized by selection: rapid heat shock of the type often imposed in the laboratory seting is likely rare in the wild. Further analysis is needed to examine to what extent such type of saturated regulatory regime is pervasive.

Our observation that co-expression increases with the onset of two stresses in rice is seemingly inconsistent with a recent study which used gene expression data collected from human monocytes to infer population correlation among transcripts (Lea et al. 2019). Several other studies have likewise reported that environmental perturbation may lead to declining co-expression (Southworth et al. 2009, Anglani et al. 2014). From a quantitative genetic perspective, a commonly observed result is that phenotypic integration in a population (i.e., the number of significant correlations among traits) increases with environmental stress (Waitt and Levin 1993, Schlichting 1989, Gianoli 2004, García-Verdugo et al. 2009). However, the stress-induced decanalization theory (Gibson 2009) suggest that new mutations or stressful environments may disrupt fine-tuned connections in a transcriptional network (Lea et al. 2019). Notably, decanalization has been hypothesized to explain complex traits and human disease (Hu et al. 2016). The degree of stress imposed on the system may dictate whether coherence (or integration) as opposed to decoherence is observed. A possible reconciliation between our results and the decoherence reported by Lea et al, may be that the monocytes studied by Lea et al. experienced a relatively more stressful environment than the rice plants studied by Wilkins et al. Indeed, we recently showed that trait co-variances vary considerably along a single environmental index (Monroe et al. 2021).

Plant response to many environmental stressors is physiologically complex (Bohnert et al. 1995) and often species-specific (Bouzid et al. 2019). Response to soil drying (drought) is representative of this complex and variable etiology, with considerable among and even within species diversity in the proximate mechanisms of response (Bouzid et al. 2019, Des Marais et al. 2012). Despite the apparently poor conservation of function among orthologs of evolutionarily distant species (Nehrt et al. 2011), newly sequenced genomes are often annotated functionally by sequence identity to distantly related reference genomes such as *Arabidopsis thaliana*. While gene expression data generated from controlled experiments on the species of interest can help to improve the accuracy of gene annotations

and therefore functional inference, many important functional relationships can be missed by the contrasting environment RNA-Seq studies that are most often employed for annotation (e.g. (Kilian et al. 2007)). The analysis presented here provides the means to identify candidate regulatory genes without the experimental challenges and costs of ChIP-Seq, mutant screens, or protein-protein interaction approaches that are commonly employed in model species.

4 Materials and Methods

4.1 Data retrieval

We utilized a TRN prior previously constructed by Wilkins et al. (2016), which was obtained from the integration of ATAC-seq (Assay for Transposase-Accessible Chromatin using sequencing) data and the CIS-BP database of TF binding motif (Weirauch et al. 2014). We elected not to use their complete "Environmental Gene Regulatory Influence Network" because the estimation of the final network relied on information from mRNA-seq time series data; the analyses presented here represent a unique approach to analyzing these data. Genes that had corresponding *cis*-regulatory elements of TF in a region of open chromatin in their promoter regions are identified as the target gene for a given TF (Wilkins et al. 2016). Note that the open accessible regulatory region derived from ATAC-seq of rice leaves remained stable across multiple environmental conditions in the Wilkins et al study. In total, this "network prior" has 38,137 interactions: 357 TFs were inferred to interact with 3240 target genes. Interactions can be between TFs and non-TF targets, or between two TFs.

The RNA-seq data derive from chamber-grown plants and were retrieved from the Gene Expression Omnibus (`www.ncbi.nlm.nih.gov/geo/`) under accession number GSE74793. This dataset comprises time-coursed libraries for four rice cultivars exposed to control (benign), heat shock, and water deficit conditions. Samples were collected with 15 min intervals for up to 4h for each of the treatments; specifically, 18 time points for controlled conditions; 9 time points for drought treatment; and 16 time points for heat treatment. Here we used a time window of nine time points in each condition for analysis. TF family annotations were downloaded from the Plant TF database (Riaño-Pachón et al. 2007), from which Heat Shock Factors are those with the TF family label "HSF". "Known" drought-related TFs were obtained from `https://funricegenes.github.io/` in June 2020 using the search terms "drought", "ABA", and "drought tolerance".

4.2 Temporal correlations for regulator-target pairs

The expression relationship observed between genes in a time series sample may be caused by the time lag inherent in molecular interactions, in this case, transcriptional regulation. Such time lag reflects the time required for a TF's activity to influence the expression of its target genes because transcription and translation take place over non-negligible time periods. Traditional correlation coefficients (e.g., Pearson correlation) cannot account for the staggered relationship between a regulator and a target. Here we used a metric we call Max Cross Correlation (MCC), building on the cross-correlation between transcript abundances estimated by RNA-Seq, to examine the activities of regulatory interactions. The MCC over the time course has a direction constraint (from regulator to target) for evaluating the regulatory status. Consider two discrete time series denoting $f(t)$ (regulator) and $g(t)$ (target), both of length of N number of time points, the cross-correlation function is defined as:

$$S_{f,g}(\tau) = \begin{cases} \frac{1}{N-\tau} \sum_{n=0}^{N-|\tau|-1} \tilde{f}(n+\tau)\tilde{g}(n), & \tau \geq 0 \\ S_{g,f}(-\tau), & \tau < 0 \end{cases} \tag{1}$$

where the $\tilde{f}(n)$ is a normalized time series (zero mean, unit variance). The maximum cross correlation $S_{f,g}(\tau)$ is calculated under condition of $m \leq \tau \leq 0$, where m is the max delay. The time delay that possesses the max correlation is defined as τ_{reg}, representing the approximate time delay that occurs between a given regulatory-target pair. The max delay is set as 1, which in the current dataset represents a 15 min time interval. . For comparison between maximum cross correlation distributions under multiple conditions, we used a Kolmogorov-Smirnov test using the *ks.test* function in *R*. Note that it is unknown to what extent of the temporal resolution the present method is effective in revealing the transient dynamic of the regulatory activity (the sampling interval in our dataset is 15 min).

4.3 Simulations for the minimal activation model

To illustrate the potential bias in capturing changing regulatory activities by using population level correlation, we implement simulation through a minimal activation model.

The rate of production of TF X and gene Y (Fig. 2A) is described by the following equation:

$$[\dot{X}] = \frac{\beta_x S_x}{1+S_x} + \beta_{basal} - d_x[X], \tag{2}$$

$$[\dot{Y}] = \frac{\beta_y (\frac{[X]}{k_x})^n}{1+(\frac{[X]}{k_x})^n} + \beta_{basal} - d_y[Y]. \tag{3}$$

$[X]$ and $[Y]$ denote the mRNA concentrations of TF X and gene Y respectively. TF X affects the transcription of gene Y. The regulated expression of genes is represented by Hill function with cooperativity exponent n. Each transcript is assumed to degrade at a rate proportional to its own concentration (d_x and d_y). Assume that the basal synthesis rate for X and Y is constant and equal with β_{basal}. β_y can be taken as the maximum strength of regulations. The stochastic dynamics of the system are implemented through Gillespie stochastic simulation algorithm (Gillespie 1977). The Hill function has the non-linear and ultrasensitivity property. By tuning the binding affinity K_x and the Hill coefficient n in models of gene regulation, we can manipulate the active range of regulatory interactions. A set of parameters including the induction signal strength S_x are determined to enable two regulatory regimes (Fig. 2C and 2F). Two types of perturbation imposed on cells at steady state are simulated, including press and pulse perturbations (Fig 2B). The press perturbation maintains the external signal at a certain high level throughout the time course, whereas the pulse perturbation indicates a discrete, transient induction of the external signal. We assume the external perturbation modulates the gene expression dynamics by the signal S_x.

Temporal dynamics of TF X and gene Y were simulated for 100 times. The cross-correlation function is calculated for the bulk time series of X and Y (average of 100 simulations), whereas the population-level Pearson's correlation coefficient (PCC) is calculated at each time point by using 100 simulations during the simulation.

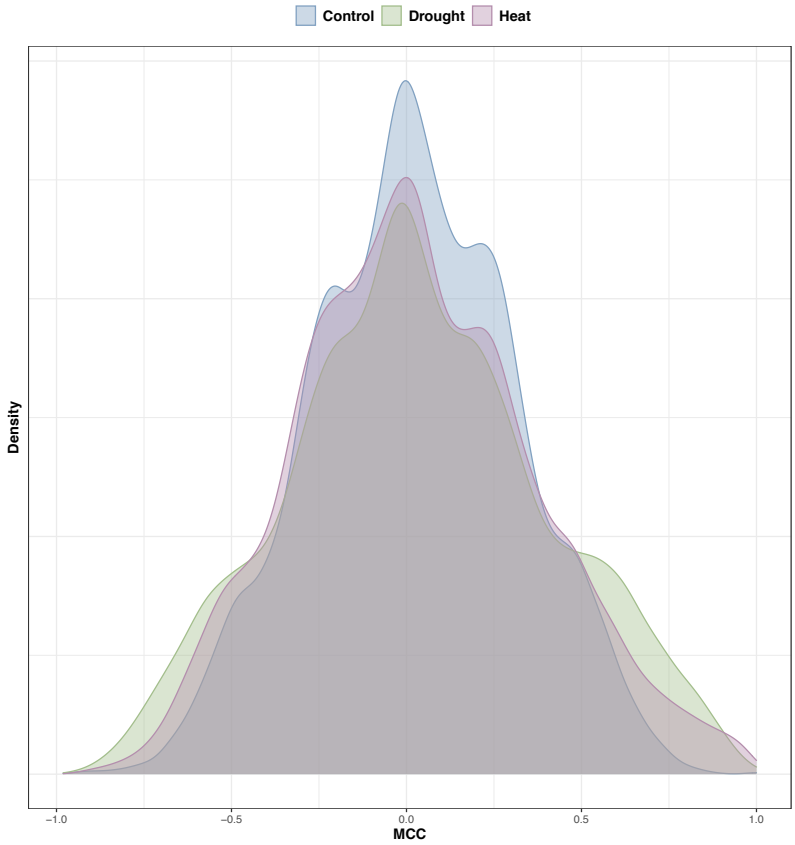

Figure 1: **Temporal correlations under multiple environmental conditions show regulatory coherence** Temporal correlation is caculated as the Max Cross Correlation (with lag ≤ 1, see Methods) for each pair of transcripts, using a previously constructed static network prior. The data comprise four rice cultivars grown under control, dehydration stress, or elevated temperature conditions, and here we analyze the data by condition over a time duration of 135 minutes following the incidence of stress. Calculated Maximum Cross Correlations (MCC) from all four cultivars were merged stress-wise.

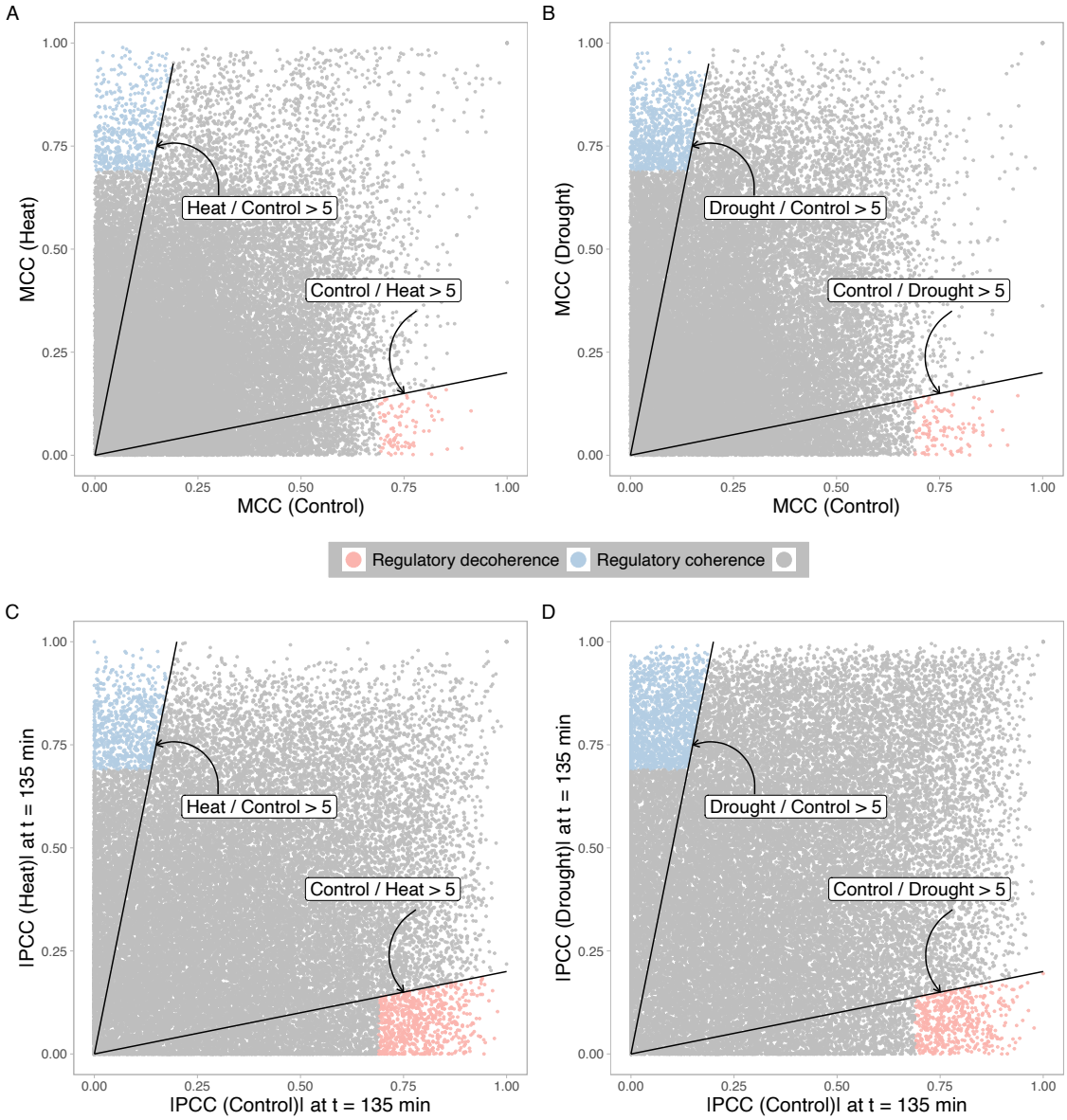

Figure 2: **Environmental perturbations lead to contrasting patterns using temporal and population correlation. A.** Comparison of the temporal correlation (Max Cross Correlation, MCC) for each regulator-target pair under control condition against heat condition. **B.** Comparison of the temporal correlation (MCC) for each regulator-target pair under control condition against soil drying condition. **C.** and **D.** show the Pearson Correlation Coefficient (PCC) of each regulator-target pair at 135 min after heat (**C**) and drought (**D**) treatment. The regulator-target pairs that are not significant in both conditions are in grey, for which the cutoff is 0.69 (p-value = 0.01). Red and blue labels highlight the pairs that show regulatory decoherence and regulatory coherence, respectively. Solid lines indicate that the ratio between regulatory scores under control and perturbed conditions is larger than 5.

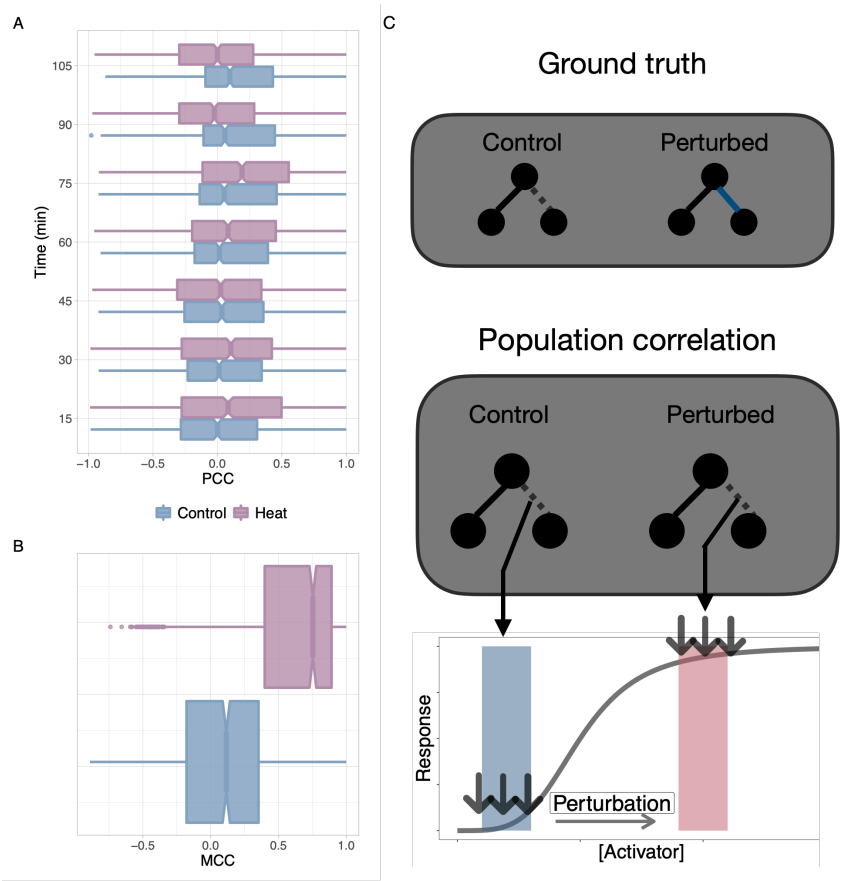

Figure 3: **Heat shock regulon shows strong contrasting patterns upon heat shock treatment. A.** Pearson Correlation Coefficient (PCC) under control and heat condition within heat shock regulon over the time course. Each boxplot represents the distribution of PCC under a given time and treatment. **B.** Max Cross Correlation (MCC) within the heat shock regulon. Genes in the heat shock regulon are identified by extracting links that include a regulator from the Heat Shock Family (HSF). As a family, HSFs have been demonstrated previously to show an important role in regulating genome-wide responses to elevated temperature in diverse species (Wang et al. 2004, Ohama et al. 2017). **C.** A schematic diagram depicts possible explanation of the temporal bias through regulatory saturation. The blue link is activated upon the perturbation (ground truth) by increasing the concentration of the regulator (an activator). However, if the dose-response curve is a sigmoid shape function, chances are the population correlation may not be able to detect such activation.

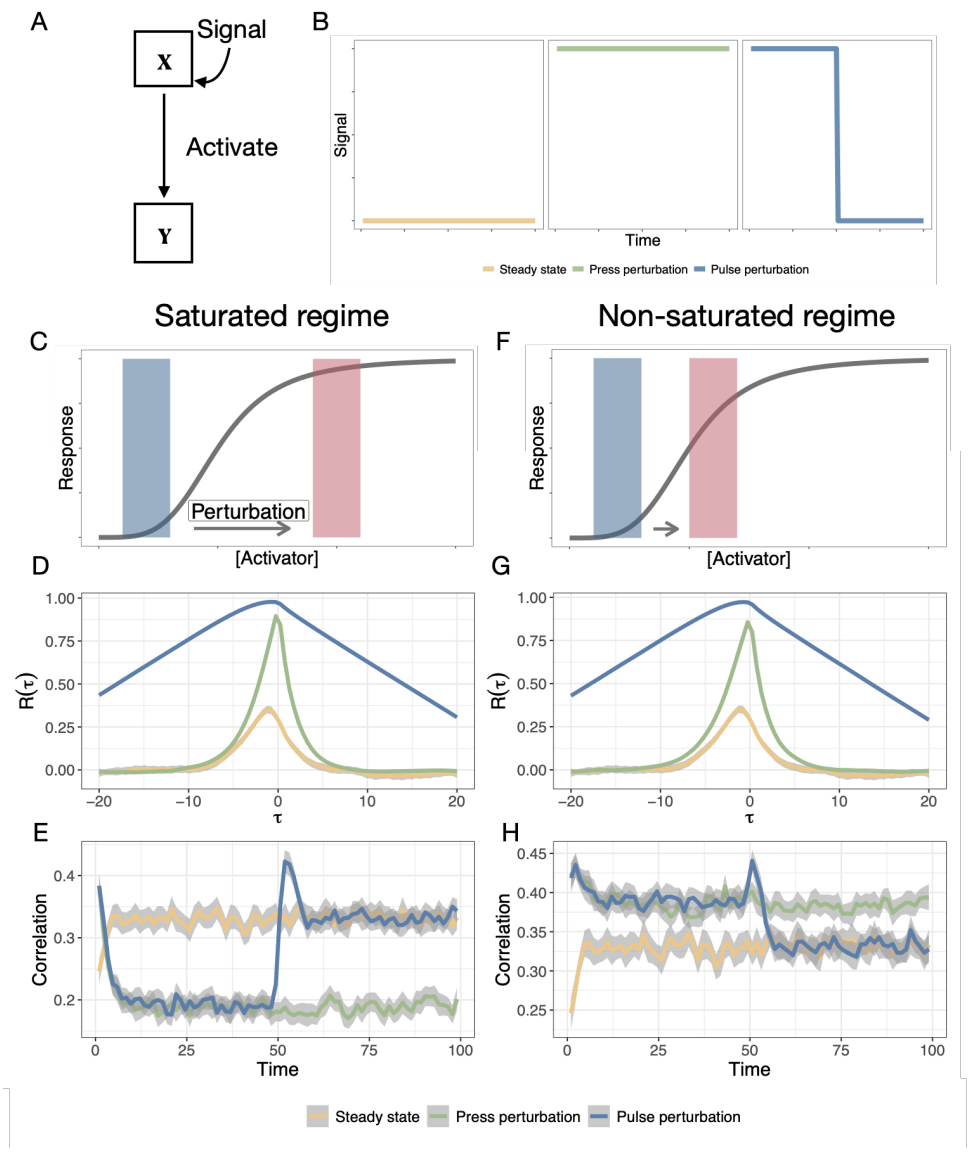

Figure 4: **Illustrated examples through stochastic simulation indicate the robustness of using temporal correlation to detect regulatory coherence.** The population level correlation may lead to temporal bias in detecting regulatory coherence depending on the regulatory regime. **A**. A schematic illustration of the minimal activation model explored here and **B**. input signals corresponding to three perturbation scenarios. **C - E**. The cross correlation function and population-level correlation between activator X and target Y under a saturated regime. The cross correlation function robustly reveals a peak in response to perturbations while the perturbation may lead to reduction of correlation when using population correlation over the time course. **F - H**. The cross correlation function and population-level correlation between activator X and target Y under a non-saturated regime. Under a non-saturated regime, both the population correlation and the temporal correlation can detect elevated level of coexpression. Colors represent three different types of external environmental conditions which lead to internal signaling (Steady state, press perturbation, and pulse perturbation). $R(\tau)$ is the cross correlation function with τ indicating the time delay. Note that the perturbation is imposed at $t = 0$ in **E** and **H**.

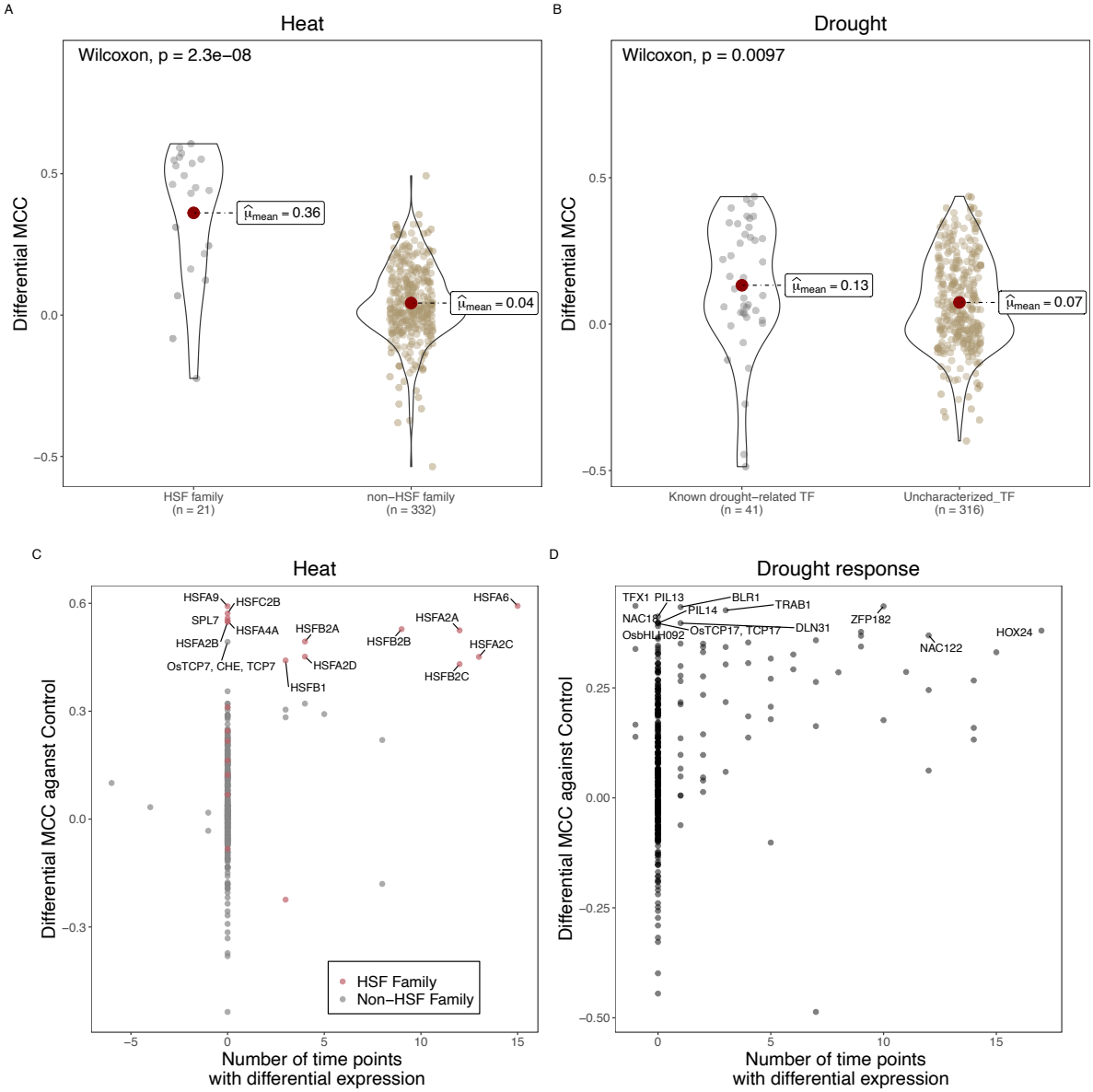

Figure 5: **Temporal correlation reveals putative key regulators of stress response.** **A.** The average differential Max Correlation Coefficient (MCC) for each regulator in the network prior under heat condition. Violin plots show members of the HSF family TF and non-HSF family TF, respectively. **B.** The average differential MCC for each regulator in the network prior under drought condition. Known drought-related TFs were obtained from `https://funricegenes.github.io/`, where genes linked with keywords "drought", "ABA", and "drought tolerance" were extracted. The average differential MCC is calculated as the averaged MCC changed across conditions. The comparison of heat **C.** and drought **D.** differential expression (the number of time points showing differential expression from the original Wilkins et al. analysis) versus differential MCC. Salmon points denote the Heat Shock Family (HSF) regulators. The number of time points with differential expression is counted for each time point and each genotypes (Maximum number is $4 * 16 = 64$). Negative numbers on the x-axis indicate number of time points in which the gene was observed to be downregulated as compared to control conditions.

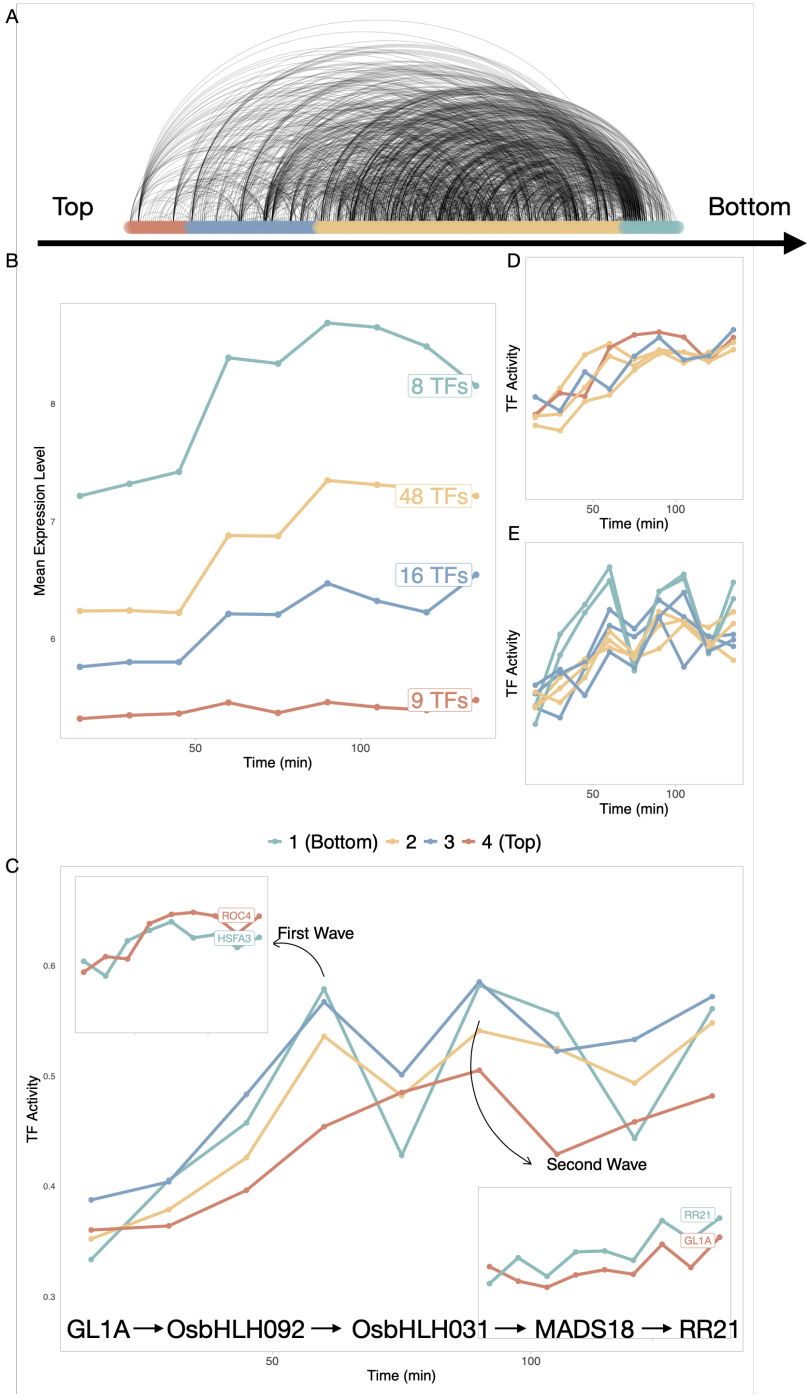

Figure 6: **Population correlation over time characterizing the dynamics of Transcription Factor activities under dehydration in a regulatory network hierarchy. A.** The hierarchical structure of the network prior constructed by a generalized bottom-up approach. Each curve represents a regulatory interaction in the network prior. The color indicates the level of a Transcription Factor (TF) in the hierarchy from top (left) to bottom (right) **B.** Comparison of mean expression value of responsive TFs in the network hierarchy. The label of each line shows the number of TFs within each level. **C.** Dynamic TF activities calculated by average population Pearson Correlation Coefficients of a TF with all its target genes. Two waves of TF activity can be observed; we thus clustered all the TF's activity within the hierarchy over time with the assistant of STEM (Ernst and Bar-Joseph 2006). Four distinct patterns are shown: 1) Continuously increasing **D**; 2). ; Two groups of TFs drive the first and second regulatory wave separately **Insets.** of **C.**. The shortest path in the **C** shows the regulatory cascade driving the second regulatory wave.

References

Alon, U., 2019. An introduction to systems biology: design principles of biological circuits. CRC press.

Alvarez-Fernandez, R., Penfold, C. A., Galvez-Valdivieso, G., Exposito-Rodriguez, M., Stallard, E. J., Bowden, L., Moore, J. D., Mead, A., Davey, P. A., Matthews, J. S., et al. 2020. Time series transcriptomics reveals a bbx32-directed control of dynamic acclimation to high light in mature arabidopsis leaves. bioRxiv .

Amar, D., Safer, H., and Shamir, R. 2013. Dissection of regulatory networks that are altered in disease via differential co-expression. PLoS computational biology 9.

Anglani, R., Creanza, T. M., Liuzzi, V. C., Piepoli, A., Panza, A., Andriulli, A., and Ancona, N. 2014. Loss of connectivity in cancer co-expression networks. PloS one 9.

Bar-Joseph, Z., Gitter, A., and Simon, I. 2012. Studying and modelling dynamic biological processes using time-series gene expression data. Nature Reviews Genetics 13:552–564.

Barzel, B. and Barabási, A.-L. 2013. Network link prediction by global silencing of indirect correlations. Nature biotechnology 31:720–725.

Bechtold, U., Penfold, C. A., Jenkins, D. J., Legaie, R., Moore, J. D., Lawson, T., Matthews, J. S., Vialet-Chabrand, S. R., Baxter, L., Subramaniam, S., et al. 2016. Time-series transcriptomics reveals that agamous-like22 affects primary metabolism and developmental processes in drought-stressed arabidopsis. The Plant Cell 28:345–366.

Bhar, A., Haubrock, M., Mukhopadhyay, A., Maulik, U., Bandyopadhyay, S., and Wingender, E. 2013. Coexpression and coregulation analysis of time-series gene expression data in estrogen-induced breast cancer cell. Algorithms for molecular biology 8:1–11.

Bhattacharjee, A., Srivastava, P. L., Nath, O., and Jain, M. 2021. Genome-wide discovery of oshox24-binding sites and regulation of desiccation stress response in rice. Plant Molecular Biology 105:205–214.

Bohnert, H. J., Nelson, D. E., and Jensen, R. G. 1995. Adaptations to environmental stresses. The plant cell 7:1099.

Bouzid, M., He, F., Schmitz, G., Häusler, R., Weber, A., Mettler-Altmann, T., and De Meaux, J. 2019. Arabidopsis species deploy distinct strategies to cope with drought stress. Annals of botany 124:27–40.

Briat, C., Gupta, A., and Khammash, M. 2016. Antithetic integral feedback ensures robust perfect adaptation in noisy biomolecular networks. Cell systems 2:15–26.

Buchanan, M., Caldarelli, G., De Los Rios, P., Rao, F., and Vendruscolo, M., 2010. Networks in cell biology. Cambridge University Press.

Buckley, T. N. 2005. The control of stomata by water balance. New phytologist 168:275–292.

Chang, K. N., Zhong, S., Weirauch, M. T., Hon, G., Pelizzola, M., Li, H., Huang, S.-s. C., Schmitz, R. J., Urich, M. A., Kuo, D., et al. 2013. Temporal transcriptional response to ethylene gas drives growth hormone cross-regulation in arabidopsis. elife 2:e00675.

Chen, Y., Li, C., Yi, J., Yang, Y., Lei, C., and Gong, M. 2020. Transcriptome response to drought, rehydration and re-dehydration in potato. International journal of molecular sciences 21:159.

Cho, S. B., Kim, J., and Kim, J. H. 2009. Identifying set-wise differential co-expression in gene expression microarray data. BMC bioinformatics 10:109.

Choi, J. K., Yu, U., Yoo, O. J., and Kim, S. 2005. Differential coexpression analysis using microarray data and its application to human cancer. Bioinformatics 21:4348–4355.

Chu, D., Zabet, N. R., and Mitavskiy, B. 2009. Models of transcription factor binding: sensitivity of activation functions to model assumptions. Journal of Theoretical Biology 257:419–429.

Cortijo, S., Bhattarai, M., Locke, J. C., and Ahnert, S. E. 2020. Co-expression networks from gene expression variability between genetically identical seedlings can reveal novel regulatory relationships. Frontiers in plant science 11.

Cuadrado, A., Manda, G., Hassan, A., Alcaraz, M. J., Barbas, C., Daiber, A., Ghezzi, P., León, R., López, M. G., Oliva, B., et al. 2018. Transcription factor nrf2 as a therapeutic target for chronic diseases: a systems medicine approach. Pharmacological reviews 70:348–383.

de la Fuente, A. 2010. From 'differential expression'to 'differential networking'–identification of dysfunctional regulatory networks in diseases. Trends in genetics 26:326–333.

Deng, S.-P., Zhu, L., and Huang, D.-S., 2015. Mining the bladder cancer-associated genes by an integrated strategy for the construction and analysis of differential co-expression networks. *in* BMC genomics, volume 16, page S4. BioMed Central.

Des Marais, D. L., McKay, J. K., Richards, J. H., Sen, S., Wayne, T., and Juenger, T. E. 2012. Physiological genomics of response to soil drying in diverse arabidopsis accessions. The Plant Cell 24:893–914.

Dunlop, M. J., Cox, R. S., Levine, J. H., Murray, R. M., and Elowitz, M. B. 2008. Regulatory activity revealed by dynamic correlations in gene expression noise. Nature genetics 40:1493–1498.

Ernst, J. and Bar-Joseph, Z. 2006. Stem: a tool for the analysis of short time series gene expression data. BMC bioinformatics 7:1–11.

Ernst, J., Vainas, O., Harbison, C. T., Simon, I., and Bar-Joseph, Z. 2007. Reconstructing dynamic regulatory maps. Molecular systems biology 3:74.

Feizi, S., Marbach, D., Médard, M., and Kellis, M. 2013. Network deconvolution as a general method to distinguish direct dependencies in networks. Nature biotechnology 31:726–733.

Ferrari, C., Proost, S., Ruprecht, C., and Mutwil, M. 2018. Phytonet: comparative co-expression network analyses across phytoplankton and land plants. Nucleic acids research 46:W76–W83.

Fiannaca, A., La Rosa, M., La Paglia, L., Rizzo, R., and Urso, A. 2015. Analysis of mirna expression profiles in breast cancer using biclustering. BMC bioinformatics 16:1–11.

Fukushima, A. 2013. Diffcorr: an r package to analyze and visualize differential correlations in biological networks. Gene 518:209–214.

Fukushima, A., Nishizawa, T., Hayakumo, M., Hikosaka, S., Saito, K., Goto, E., and Kusano, M. 2012. Exploring tomato gene functions based on coexpression modules using graph clustering and differential coexpression approaches. Plant physiology 158:1487–1502.

Gao, C., McDowell, I. C., Zhao, S., Brown, C. D., and Engelhardt, B. E. 2016. Context specific and differential gene co-expression networks via bayesian biclustering. PLoS computational biology 12:e1004791.

Gao, Q., Ho, C., Jia, Y., Li, J. J., and Huang, H. 2012. Bi c lustering of li near p atterns in gene expression data. Journal of Computational Biology 19:619–631.

Garber, M., Yosef, N., Goren, A., Raychowdhury, R., Thielke, A., Guttman, M., Robinson, J., Minie, B., Chevrier, N., Itzhaki, Z., et al. 2012. A high-throughput chromatin immunoprecipitation approach reveals principles of dynamic gene regulation in mammals. Molecular cell 47:810–822.

García-Verdugo, C., Granado-Yela, C., Manrique, E., Rubio de Casas, R., and Balaguer, L. 2009. Phenotypic plasticity and integration across the canopy of olea europaea subsp. guanchica (oleaceae) in populations with different wind exposures. American Journal of Botany 96:1454–1461.

Gargouri, M., Park, J.-J., Holguin, F. O., Kim, M.-J., Wang, H., Deshpande, R. R., Shachar-Hill, Y., Hicks, L. M., and Gang, D. R. 2015. Identification of regulatory network hubs that control lipid metabolism in chlamydomonas reinhardtii. Journal of experimental botany 66:4551–4566.

Gerstein, M. B., Kundaje, A., Hariharan, M., Landt, S. G., Yan, K.-K., Cheng, C., Mu, X. J., Khurana, E., Rozowsky, J., Alexander, R., et al. 2012. Architecture of the human regulatory network derived from encode data. Nature 489:91–100.

Gianoli, E. 2004. Plasticity of traits and correlations in two populations of convolvulus arvensis (convolvulaceae) differing in environmental heterogeneity. International Journal of Plant Sciences 165:825–832.

Gibson, G. 2008. The environmental contribution to gene expression profiles. Nature reviews genetics 9:575–581.

Gibson, G. 2009. Decanalization and the origin of complex disease. Nature Reviews Genetics 10:134–140.

Gillespie, D. T. 1977. Exact stochastic simulation of coupled chemical reactions. The journal of physical chemistry 81:2340–2361.

Greenham, K., Guadagno, C. R., Gehan, M. A., Mockler, T. C., Weinig, C., Ewers, B. E., and McClung, C. R. 2017. Temporal network analysis identifies early physiological and transcriptomic indicators of mild drought in brassica rapa. Elife 6:e29655.

Hirata, H., Yoshiura, S., Ohtsuka, T., Bessho, Y., Harada, T., Yoshikawa, K., and Kageyama, R. 2002. Oscillatory expression of the bhlh factor hes1 regulated by a negative feedback loop. Science 298:840–843.

Hu, J. X., Thomas, C. E., and Brunak, S. 2016. Network biology concepts in complex disease comorbidities. Nature Reviews Genetics 17:615.

Hu, R., Qiu, X., Glazko, G., Klebanov, L., and Yakovlev, A. 2009. Detecting intergene correlation changes in microarray analysis: a new approach to gene selection. BMC bioinformatics 10:1–9.

Huang, J., Sun, S., Xu, D., Lan, H., Sun, H., Wang, Z., Bao, Y., Wang, J., Tang, H., and Zhang, H. 2012. A tfiiia-type zinc finger protein confers multiple abiotic stress tolerances in transgenic rice (oryza sativa l.). Plant molecular biology 80:337–350.

Hudson, N. J., Reverter, A., and Dalrymple, B. P. 2009. A differential wiring analysis of expression data correctly identifies the gene containing the causal mutation. PLoS computational biology 5:e1000382.

Joshi, R., Wani, S. H., Singh, B., Bohra, A., Dar, Z. A., Lone, A. A., Pareek, A., and Singla-Pareek, S. L. 2016. Transcription factors and plants response to drought stress: current understanding and future directions. Frontiers in Plant Science 7:1029.

Kilian, J., Whitehead, D., Horak, J., Wanke, D., Weinl, S., Batistic, O., D'Angelo, C., Bornberg-Bauer, E., Kudla, J., and Harter, K. 2007. The atgenexpress global stress expression data set: protocols, evaluation and model data analysis of uv-b light, drought and cold stress responses. The Plant Journal 50:347–363.

Kostka, D. and Spang, R. 2004. Finding disease specific alterations in the co-expression of genes. Bioinformatics 20:i194–i199.

Lan Thi Hoang, X., Du Nhi, N. H., Binh Anh Thu, N., Phuong Thao, N., and Phan Tran, L.-S. 2017. Transcription factors and their roles in signal transduction in plants under abiotic stresses. Current genomics 18:483–497.

Langfelder, P. and Horvath, S. 2008. Wgcna: an r package for weighted correlation network analysis. BMC bioinformatics 9:559.

Lea, A., Subramaniam, M., Ko, A., Lehtimäki, T., Raitoharju, E., Kähönen, M., Seppälä, I., Mononen, N., Raitakari, O. T., Ala-Korpela, M., et al. 2019. Genetic and environmental perturbations lead to regulatory decoherence. eLife 8:e40538.

Lee, T. I. and Young, R. A. 2013. Transcriptional regulation and its misregulation in disease. Cell 152:1237–1251.

Lewis, J. 2003. Autoinhibition with transcriptional delay: a simple mechanism for the zebrafish somitogenesis oscillator. Current Biology 13:1398–1408.

Li, P., Yang, H., Wang, L., Liu, H., Huo, H., Zhang, C., Liu, A., Zhu, A., Hu, J., Lin, Y., et al. 2019. Physiological and transcriptome analyses reveal short-term responses and formation of memory under drought stress in rice. Frontiers in genetics 10:55.

Love, M. I., Huber, W., and Anders, S. 2014. Moderated estimation of fold change and dispersion for rna-seq data with deseq2. Genome biology 15:1–21.

Luscombe, N. M., Babu, M. M., Yu, H., Snyder, M., Teichmann, S. A., and Gerstein, M. 2004. Genomic analysis of regulatory network dynamics reveals large topological changes. Nature 431:308–312.

Ma, W., Trusina, A., El-Samad, H., Lim, W. A., and Tang, C. 2009. Defining network topologies that can achieve biochemical adaptation. Cell 138:760–773.

Manna, M., Thakur, T., Chirom, O., Mandlik, R., Deshmukh, R., and Salvi, P. 2020. Transcription factors as key molecular target to strengthen the drought stress tolerance in plants. Physiologia Plantarum .

Martín-Trillo, M. and Cubas, P. 2010. Tcp genes: a family snapshot ten years later. Trends in plant science 15:31–39.

Monaco, G., van Dam, S., Ribeiro, J. L. C. N., Larbi, A., and de Magalhães, J. P. 2015. A comparison of human and mouse gene co-expression networks reveals conservation and divergence at the tissue, pathway and disease levels. BMC evolutionary biology 15:1–14.

Monroe, J., Cai, H., and Des Marais, D. L. 2021. Diversity in non-linear responses to soil moisture shapes evolutionary constraints in brachypodium. G3 Genes| Genomes| Genetics .

Müller, M., Seifert, S., Lübbe, T., Leuschner, C., and Finkeldey, R. 2017. De novo transcriptome assembly and analysis of differential gene expression in response to drought in european beech. PloS one 12:e0184167.

Nakamura, Y., Kato, T., Yamashino, T., Murakami, M., and Mizuno, T. 2007. Characterization of a set of phytochrome-interacting factor-like bhlh proteins in oryza sativa. Bioscience, Biotechnology, and Biochemistry 71:1183–1191.

Neef, D. W., Jaeger, A. M., and Thiele, D. J. 2011. Heat shock transcription factor 1 as a therapeutic target in neurodegenerative diseases. Nature reviews Drug discovery 10:930–944.

Neef, D. W., Turski, M. L., and Thiele, D. J. 2010. Modulation of heat shock transcription factor 1 as a therapeutic target for small molecule intervention in neurodegenerative disease. PLoS biology 8.

Nehrt, N. L., Clark, W. T., Radivojac, P., and Hahn, M. W. 2011. Testing the ortholog conjecture with comparative functional genomic data from mammals. PLoS Comput Biol 7:e1002073.

Ni, L., Bruce, C., Hart, C., Leigh-Bell, J., Gelperin, D., Umansky, L., Gerstein, M. B., and Snyder, M. 2009. Dynamic and complex transcription factor binding during an inducible response in yeast. Genes & development 23:1351–1363.

Ohama, N., Sato, H., Shinozaki, K., and Yamaguchi-Shinozaki, K. 2017. Transcriptional regulatory network of plant heat stress response. Trends in plant science 22:53–65.

Parsana, P., Ruberman, C., Jaffe, A. E., Schatz, M. C., Battle, A., and Leek, J. T. 2019. Addressing confounding artifacts in reconstruction of gene co-expression networks. Genome biology 20:1–6.

Piggot, P. J. and Hilbert, D. W. 2004. Sporulation of bacillus subtilis. Current opinion in microbiology 7:579–586.

Rastogi, A., Maheswari, U., Dorrell, R. G., Vieira, F. R. J., Maumus, F., Kustka, A., McCarthy, J., Allen, A. E., Kersey, P., Bowler, C., et al. 2018. Integrative analysis of large scale transcriptome data draws a comprehensive landscape of phaeodactylum tricornutum genome and evolutionary origin of diatoms. Scientific reports 8:1–14.

Riaño-Pachón, D. M., Ruzicic, S., Dreyer, I., and Mueller-Roeber, B. 2007. Plntfdb: an integrative plant transcription factor database. BMC bioinformatics 8:1–10.

Ruprecht, C., Proost, S., Hernandez-Coronado, M., Ortiz-Ramirez, C., Lang, D., Rensing, S. A., Becker, J. D., Vandepoele, K., and Mutwil, M. 2017*a*. Phylogenomic analysis of gene co-expression networks reveals the evolution of functional modules. The Plant Journal 90:447–465.

Ruprecht, C., Vaid, N., Proost, S., Persson, S., and Mutwil, M. 2017*b*. Beyond genomics: studying evolution with gene coexpression networks. Trends in Plant Science 22:298–307.

Schlichting, C. D. 1989. Phenotypic integration and environmental change. BioScience 39:460.

Scott, M. S., Perkins, T., Bunnell, S., Pepin, F., Thomas, D. Y., and Hallett, M. 2005. Identifying regulatory subnetworks for a set of genes. Molecular & Cellular Proteomics 4:683–692.

Smith, H. 1990. Signal perception, differential expression within multigene families and the molecular basis of phenotypic plasticity. Plant, Cell & Environment 13:585–594.

Song, L., Huang, S.-s. C., Wise, A., Castanon, R., Nery, J. R., Chen, H., Watanabe, M., Thomas, J., Bar-Joseph, Z., and Ecker, J. R. 2016. A transcription factor hierarchy defines an environmental stress response network. Science 354:aag1550.

Southworth, L. K., Owen, A. B., and Kim, S. K. 2009. Aging mice show a decreasing correlation of gene expression within genetic modules. PLoS genetics 5.

Spampanato, C., Feeney, E., Li, L., Cardone, M., Lim, J.-A., Annunziata, F., Zare, H., Polishchuk, R., Puertollano, R., Parenti, G., et al. 2013. Transcription factor eb (tfeb) is a new therapeutic target for pompe disease. EMBO molecular medicine 5:691–706.

Tesson, B. M., Breitling, R., and Jansen, R. C. 2010. Diffcoex: a simple and sensitive method to find differentially coexpressed gene modules. BMC bioinformatics 11:1–9.

Todaka, D., Nakashima, K., Maruyama, K., Kidokoro, S., Osakabe, Y., Ito, Y., Matsukura, S., Fujita, Y., Yoshiwara, K., Ohme-Takagi, M., et al. 2012. Rice phytochrome-interacting factor-like protein ospil1 functions as a key regulator of internode elongation and induces a morphological response to drought stress. Proceedings of the National Academy of Sciences 109:15947–15952.

Toledo, F. and Wahl, G. M. 2006. Regulating the p53 pathway: in vitro hypotheses, in vivo veritas. Nature Reviews Cancer 6:909–923.

Tsai, Y.-C., Weir, N. R., Hill, K., Zhang, W., Kim, H. J., Shiu, S.-H., Schaller, G. E., and Kieber, J. J. 2012. Characterization of genes involved in cytokinin signaling and metabolism from rice. Plant Physiology 158:1666–1684.

van Dijk, D., Sharon, E., Lotan-Pompan, M., Weinberger, A., Segal, E., and Carey, L. B. 2017. Large-scale mapping of gene regulatory logic reveals context-dependent repression by transcriptional activators. Genome research 27:87–94.

Varala, K., Marshall-Colón, A., Cirrone, J., Brooks, M. D., Pasquino, A. V., Léran, S., Mittal, S., Rock, T. M., Edwards, M. B., Kim, G. J., et al. 2018. Temporal transcriptional logic of dynamic regulatory networks underlying nitrogen signaling and use in plants. Proceedings of the National Academy of Sciences 115:6494–6499.

von Koskull-Döring, P., Scharf, K.-D., and Nover, L. 2007. The diversity of plant heat stress transcription factors. Trends in plant science 12:452–457.

Waitt, D. E. and Levin, D. A. 1993. Phenotypic integration and plastic correlations in phlox drummondii (polemoniaceae). American Journal of Botany 80:1224–1233.

Wang, H., Wang, H., Shao, H., and Tang, X. 2016. Recent advances in utilizing transcription factors to improve plant abiotic stress tolerance by transgenic technology. Frontiers in plant science 7:67.

Wang, W., Vinocur, B., Shoseyov, O., and Altman, A. 2004. Role of plant heat-shock proteins and molecular chaperones in the abiotic stress response. Trends in plant science 9:244–252.

Weirauch, M. T., Yang, A., Albu, M., Cote, A. G., Montenegro-Montero, A., Drewe, P., Najafabadi, H. S., Lambert, S. A., Mann, I., Cook, K., et al. 2014. Determination and inference of eukaryotic transcription factor sequence specificity. Cell 158:1431–1443.

Wilkins, O., Hafemeister, C., Plessis, A., Holloway-Phillips, M.-M., Pham, G. M., Nicotra, A. B., Gregorio, G. B., Jagadish, S. K., Septiningsih, E. M., Bonneau, R., et al. 2016. Egrins (environmental gene regulatory influence networks) in rice that function in the response to water deficit, high temperature, and agricultural environments. The Plant Cell 28:2365–2384.

Windram, O., Madhou, P., McHattie, S., Hill, C., Hickman, R., Cooke, E., Jenkins, D. J., Penfold, C. A., Baxter, L., Breeze, E., et al. 2012. Arabidopsis defense against botrytis cinerea: chronology and regulation deciphered by high-resolution temporal transcriptomic analysis. The Plant Cell 24:3530–3557.

Wray, G. A., Hahn, M. W., Abouheif, E., Balhoff, J. P., Pizer, M., Rockman, M. V., and Romano, L. A. 2003. The evolution of transcriptional regulation in eukaryotes. Molecular biology and evolution 20:1377–1419.

Yan, Q., Wu, F., Yan, Z., Li, J., Ma, T., Zhang, Y., Zhao, Y., Wang, Y., and Zhang, J. 2019. Differential co-expression networks of long non-coding rnas and mrnas in cleistogenes songorica under water stress and during recovery. BMC plant biology 19:1–19.

Yeung, E., van Veen, H., Vashisht, D., Paiva, A. L. S., Hummel, M., Rankenberg, T., Steffens, B., Steffen-Heins, A., Sauter, M., de Vries, M., et al. 2018. A stress recovery signaling network for enhanced flooding tolerance in arabidopsis thaliana. Proceedings of the National Academy of Sciences 115:E6085–E6094.

Yu, H. and Gerstein, M. 2006. Genomic analysis of the hierarchical structure of regulatory networks. Proceedings of the National Academy of Sciences 103:14724–14731.

Yuan, W., Beaulieu-Jones, B. K., Yu, K.-H., Lipnick, S. L., Palmer, N., Loscalzo, J., Cai, T., and Kohane, I. S. 2021. Temporal bias in case-control design: preventing reliable predictions of the future. Nature Communications 12:1107. URL https://doi.org/10.1038/s41467-021-21390-2.

Zander, M., Lewsey, M. G., Clark, N. M., Yin, L., Bartlett, A., Guzmán, J. P. S., Hann, E., Langford, A. E., Jow, B., Wise, A., et al. 2020. Integrated multi-omics framework of the plant response to jasmonic acid. Nature Plants 6:290–302.

Zeisel, A., Muñoz-Manchado, A. B., Codeluppi, S., Lönnerberg, P., La Manno, G., Juréus, A., Marques, S., Munguba, H., He, L., Betsholtz, C., et al. 2015. Cell types in the mouse cortex and hippocampus revealed by single-cell rna-seq. Science 347:1138–1142.

Zheng, K., Wang, X., Wang, Y., and Wang, S. 2021. Conserved and non-conserved functions of the rice homologs of the arabidopsis trichome initiation-regulating mbw complex proteins. BMC plant biology 21:1–15.

Zinzen, R. P., Girardot, C., Gagneur, J., Braun, M., and Furlong, E. E. 2009. Combinatorial binding predicts spatio-temporal cis-regulatory activity. Nature 462:65–70.